Modeling of the electron beam induced current signal in nanowires with an axial p-n junction

Abderrezak Lahreche, Andrey V Babichev, Yamina Beggah, Maria Tchernycheva

Modeling of the electron beam induced current signal in nanowires with an axial p-n junction

Abderrezak Lahreche[1,2], Andrey V Babichev[3,4], Yamina Beggah[2] and Maria Tchernycheva[5]

[1]Department de technologie, Université A.Mira de Bejaia, 6000 Bejaia, Algérie
[2]Laboratoire Matériaux: Elaborations – Propriétés - Applications (LMEPA), Université Jijel, 18000 Jijel, Algérie
[3]Saint Petersburg Electrotechnical University "LETI", 197376 St. Petersburg, Russia
[4]ITMO University, 197101 St. Petersburg, Russia
[5]Centre de Nanosciences et de Nanotechnologies (C2N), CNRS UMR 9001, University Paris-Saclay, 91120 Palaiseau, France

E-mail: abderrezak.lahreche@univ-bejaia.dz, maria.tchernycheva@c2n.upsaclay.fr

Received xxxxxx
Accepted for publication xxxxxx
Published xxxxxx

Abstract

A tridimensional mathematical model to calculate the electron beam induced current (EBIC) of an axial p-n nanowire junction is proposed. The effect of the electron beam and junction parameters on the distribution of charge carriers and on the collected EBIC current is reported.
We demonstrate that the diffusion of charge carriers within the wire is strongly influenced by the electrical state of its lateral surface which is characterized by a parameter called surface recombination velocity (v_r). When the surface recombination is weak (i.e. low v_r value), the diffusion of charge carriers occurs in one dimension (1-D) along the wire axis, and, in this case, the use of bulk EBIC models to extract the diffusion length (L) of charge carriers is justified. However, when the surface effects are strong (i.e. high v_r values), the diffusion happens in three dimensions (3-D). In this case, the EBIC profiles depend on v_r value and two distinct cases can be defined. If the L is larger than the nanowire radius (r_a), the EBIC profiles show a strong dependency with this parameter. This gives evidence that the recombination of generated carriers on the surface through v_r is the dominant process. In this situation, a decrease of two orders of magnitude in the EBIC profiles computed with a high and a low v_r value is observed in neutral regions of the junction. For the case of L smaller than r_a the dependency of the EBIC profiles on the v_r is weak, and the prevalent recombination mechanism is the bulk recombination process.

Keywords: Modelling, Electron beam induced current microscopy, Axial nanowire p-n junction, Diffusion length, Surface recombination, Electrical nanoscale characterization.

Introduction

The characterization of the electrical properties of semiconductors is one of the most important steps in the manufacturing of electronic and optoelectronic devices. For example, an estimate of the diffusion length of charge carriers is essential to optimize the conversion energy of solar cells. Recently, scientists have begun to investigate materials in the form of thin films and nanostructures for the photovoltaic conversion in order to take advantage from their favorable optical and electrical properties. Much attention has been paid to III-V and II-VI nanowires (NWs) [1–3]. However, the nanostructuring of the active region brings new characterization challenges. Indeed, standard photovoltaic macroscopic measurements provide only values averaged over a large number of NWs, which is not always relevant for the optimization of material parameters. Nanoscale analyses probing the electrical properties of individual NWs are needed, which explains the recent regain of interest for the electron beam induced current (EBIC) microscopy applied to nanostructured devices [4].

EBIC provides easy and reliable feedback information about eventual failures in the device and allows to determine important material parameters. These are, for example, the diffusion length of the charge carriers, L, and the electrical surface states of the optoelectronic devices such as solar cells [5–10].

To determine the diffusion length, the common strategy in the literature is to fit the recorded experimental EBIC profiles with a theoretical equation of the type $I = I_{max}\, exp\left(-\frac{z}{L}\right)$ with I_{max} the maximum current, z, the distance between the point of impact of the primary beam and the collecting junction, and L, diffusion length [11–13]. This equation was initially proposed to fit the EBIC profile in bulk semiconductors with zero surface recombination velocity $v_r = 0$ (effect of surfaces is neglected). Furthermore, the use of this equation needs certain conditions to be fulfilled, e.g. $z > 2L$ and $R \ll L$ [12] where R is the electron range relationship determining the average radius of interacting volume (cf. eq. (2) below). This equation has been used by many authors to determine the L value of charge carriers for nanowire solar cells [14–26], however its validity can be open questioned. In the case of nanowires, because of their small radial dimension, the surface to the volume ratio is high, rendering surface effects not negligible. Therefore, ignoring the effect of the recombination of charge carriers on the lateral surface of the wire can induce an error in the determination of the diffusion length value. In addition, the diffusion of charge carriers can be no longer considered as one-dimensional, invalidating the use of the above-mentioned equation.

In this paper, we propose a more realistic theoretical model to describe the EBIC signal of an axial p-n nanowire junction. In this model, we take into account the effect of the length of the wire, its radius, the doping of the two regions of the junction, the width of the space charge region, the diffusion length of the charge carriers and their recombination velocity on the lateral surface of the wire. The impact of each of these parameters on the EBIC profile is discussed in detail.

2 The model

2.1 Main assumptions

Figure 1 presents typical configurations used for the EBIC experiments on the cross-sectional surface of a p-n axial nanowire junction. First configuration illustrated in panels (a) and (b) shows scanning electron miscoscope and EBIC images of a GaAsP p-n junction nanowire under investigation standing on the growthSi(111) substrate, which is grounded. The electrical connection is ensured by the nanomanipulator positioned in contact with the catalyst particle on the nanowire top [26]. Second configuration shown in panel (c) presents a nanowire after sonification and transfer on a SiO_2/Si substrate. The two extremities of the nanowire are contacted with nanomanipulators. Both experimental configurations can be schematized as illustrated in panel (d). This schematic is used in the present model. An electron beam of a given energy (from 3 to 25 keV) is focused on the wire's lateral surface which causes a creation of electron-hole pairs within a certain volume in the NW called "interaction volume". The generated carriers are drifted apart in the presence of an electric field and are collected to produce an induced current. The NW extremities are electrically connected to alock-in current amplifier and the induced current is recorded for each excitation position to construct an EBIC map (an example is shown in Figure 1(b)) or a line scan. In the following, we focus the investigation on the scans of the electron beam along the z direction corresponding to the elongated NW axis.

To theoretically determine the EBIC current I_C, we follow standard procedures. First, we solve the continuity equation with the appropriate boundary conditions to obtain the spatial distribution of excess concentration of minority charge carriers, then we compute the EBIC currentI_C value.

To find an analytical solution to the EBIC current distribution, we adopt the following assumptions:

- The injection rate of the charge carriers is low.
- Non-radiative recombination of charge carriers on lateral surface of the wire is characterized by a parameter called surface recombination velocity.
- The dopant concentration and the diffusion length of charge carriers are considered constant on the both sides of the junction.

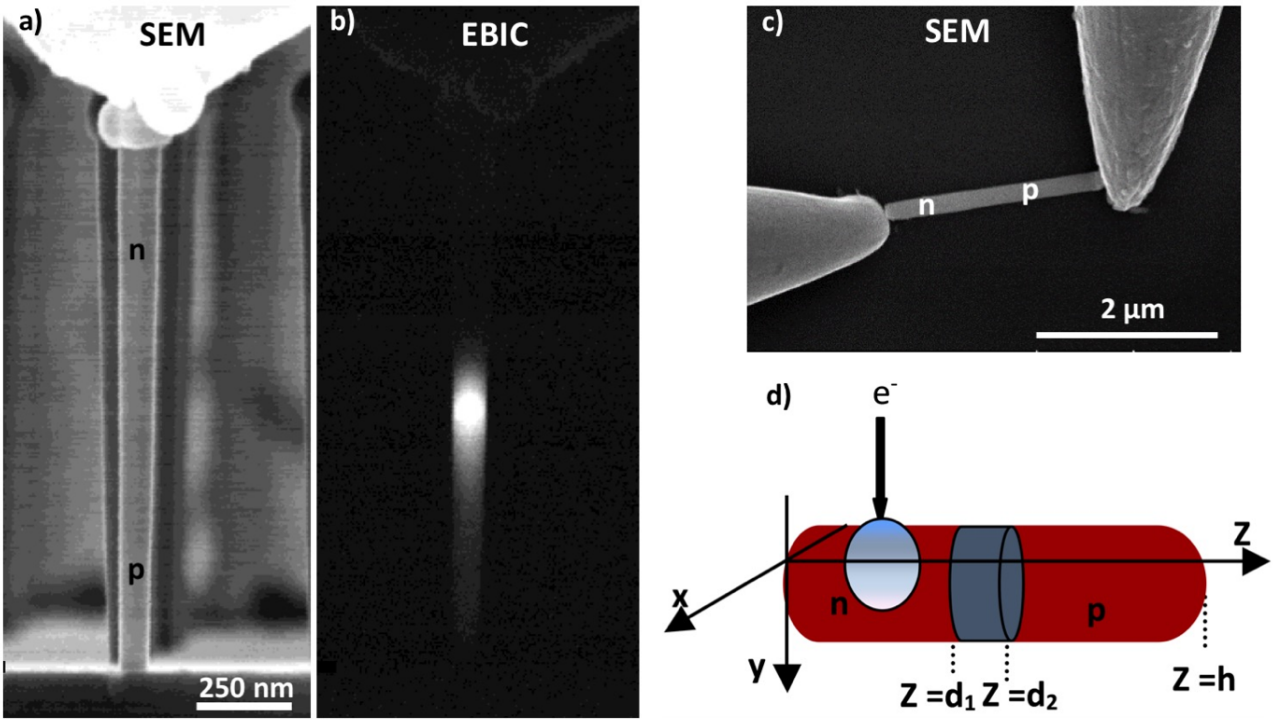

Figure 1. Typical configurations used for EBIC measurements of p-n nanowire junctions: (a) SEM and (b) EBIC images of a vertically standing nanowire, contacted with a nanomanipulator on the top catalyst particle; (c) SEM image of a lying nanowire contacted with two nanomanipulators on the extremities; (d) Schematic of the model.

- There is no recombination of charge carriers in space charge region (SCR) and in the collecting contacts at $z=d_1$and at $z=d_2$.
- The generation of excess carriers is described by [27]:

$$g(r,z) = \frac{1}{a}\exp\left(-\frac{z^2}{\sigma_1^2}\right)(r_a - r)\exp(-(r_a - r)/\sigma_2) \quad (1)$$

$$a = \sqrt{\pi}\sigma_1\sigma_2^3$$

$$\sigma_1 = \sqrt{0.05 + 0.0001E_0^{2.78}}$$

$$\sigma_2 = 0.02 + 0.003E_0^{1.50}$$

where $E_0$is the energy of the electron beam.

- The electron range R_C is given by [28]

$$R_c(\mu m) = 2.76\frac{10^{-2}A}{\rho Z^{0.889}}E_0^{1.67} \quad (2)$$

2.2 Distribution of minority charge carriers

The minority charge carrier distribution is obtained by solving diffusion equation with appropriate boundary conditions. For n-doped region we can write the hole distribution as

$$\frac{\partial^2 p(r,z)}{\partial r^2} + \frac{1}{r}\frac{\partial p(r,z)}{\partial r} + \frac{1}{r}\frac{\partial^2 p(r,z)}{\partial \theta^2} + \frac{\partial^2 p(r,z)}{\partial z^2} - \lambda^2 p(r,z) = -\frac{g(r,z)}{D_p} \quad (3)$$

$$\lambda^2 = \frac{1}{L_p},\ L_p = D_p\tau,$$

where $D_p$is the diffusion coefficient of holes.

With boundary conditions:

$$p(r, z = 0) = 0 \quad (4\text{-a})$$

$$p(r, z = d_1) = 0 \quad (4\text{-b})$$

$$D_p\frac{\partial p}{\partial r}(r = r_a, z) = -v_p.p(r = r_a, z) \quad (4\text{-c})$$

And for the p-doped region the electron concentration should satisfy the equation:

$$\frac{\partial^2 n(r,z)}{\partial r^2} + \frac{1}{r}\frac{\partial n(r,z)}{\partial r} + \frac{1}{r}\frac{\partial^2 n(r,z)}{\partial \theta^2} + \frac{\partial^2 n(r,z)}{\partial z^2} - \lambda'^2 n(r,z) = -\frac{g(r,z)}{D_n} \quad (5)$$

$$\lambda'^2 = \frac{1}{L_n},\ L_n = D_n\tau,$$

where D_n is the diffusion coefficient of electrons.

Boundary conditions are:

$$n(r, z = d_2) = 0 \quad (6\text{-a})$$

$$n(r, z = h) = 0 \quad (6\text{-b})$$

$$D_n\frac{\partial n}{\partial r}(r = r_a, z) = -v_n.p(r = r_a, z) \quad (6\text{-c})$$

A solution of the diffusion equations (3) and (5) accounting for the boundaries conditions can be obtained using standard mathematical methods. Using the Green function formalism [29] one can obtain:

$$q(r,z) = \iint G(r,r',z,z').g(r',z'-z_0)dr'dz'd\theta' \quad (7)$$

where $q(r,z)$ is the charge carrier concentration in the corresponding region, i.e. it corresponds to p in n-doped region and to n in p-doped region of the junction,

$G(r,r',z,z')$is the Green function and $g(r',z'-z_0)$ is the generation function.

In the n-doped region, the Green function writes:

$$G(r,r',z,z') = \frac{1}{2\pi D}\sum_{i=1}^{n} \frac{2}{r_a^2.\left(J_0{}^2(k_i.r_a^2)+J_1{}^2(k_i.r_a^2)\right)}.J_0(k_i r).J_0(k_i r').\frac{1}{\mu_i.sinh(\mu_i.d_1)}[\sin h(\mu_i z_>).\sin h(\mu_i(d_1-z_<)] \quad (8)$$

k_i is the solution of transactional equation

$$k_i J_1(k_i.r_a) = s_p J_0(k_i.r_a) \quad (9)$$

$$s_p = \frac{v_p}{D_p} \text{and} \mu_p = \sqrt{k_i^2 + L_p^{-2}}$$

$$z_> = \max(z,z'), \qquad z_< = \min(z,z')$$

$J_0$and J_1 are the Bessel functions of order 0 and 1, respectively.

Similarly, in the p-doped region:

$$G(r,r',z,z') = \frac{1}{2\pi D}\sum_{i=1}^{n} \frac{2}{r_a^2.\left(J_0{}^2(k_i.r_a^2)+J_1{}^2(k_i.r_a^2)\right)}.J_0(k_i r).J_0(k_i r').\frac{1}{\mu_i.sinh(\mu_i.(h-d_2))}[\sinh(\mu_i(h-z_<)).\sinh(\mu_i(d_2-z_<)] \quad (10)$$

k_i is the solution of transactional equation

$$k_i J_1(k_i.r_a) = s_n J_0(k_i.r_a) \quad (11)$$

$$s_n = \frac{v_n}{D_n} \text{and} \mu_n = \sqrt{k_i^2 + L_n^{-2}}$$

$$z_> = \max(z,z'), \qquad z_< = \min(z,z')$$

$J_0$and J_1 are the Bessel functions of order 0 and 1, respectively.

2.3 The EBIC current

The I_C current is considered to be a sum of the three currents generated in the three parts of the junction: the neutral p-doped part (p region), the neutral n-doped part (n region) and the space charge region (SCR), noted I_{CP}, $I_{CN}$and I_{SCR} respectively:

$$I_C = I_{CN} + I_{SCR} + I_{CP} \quad (12)$$

I_{CN}: Minority charge carrier current in p-doped region;

I_{CP}: Minority charge carrier current in n-doped region;

I_{SCR}: The current of SCR.

The EBIC current in the n- and p-doped regions is given by:

$$I_{CN} = -eD\int_0^{r_a} r dr \int_0^{2\pi} d\theta \left.\frac{\partial n}{\partial z}\right|_{z=d_1} \quad (13)$$

$$I_{CP} = eD\int_0^{r_a} r dr \int_0^{2\pi} d\theta \left.\frac{\partial p}{\partial z}\right|_{z=d_2} \quad (14)$$

As for the SCR, the generated charge carriers in this region are immediately separated by the built-in electric field and therefore participate in the formation of the EBIC signal:

$$I_{SCR} = 2\pi\int_0^{r_a}\int_{d_2}^{d_2} g(r,z-z_0)dzdr \quad (15)$$

3 Results

3.1 Charge carriers distribution

Surface recombination velocity v_r plays an important role on the distribution of the concentration $p(r,z)$. For small v_r values, the distribution of the charge carriers depends only on the z direction as illustrated in figure 2(a), (c), (e) and (g). For a diffusion length $L_p<r_a$, the generated minority carriers are chiefly located near the generation volume and have a spatial extension of R_C along the z axis. For $L_p>r_a$, the extension of the generated minority carriers in the z direction becomes more noticeable. As a function of z (while z remains smaller than the wire length h), the decrease has an exponential shape as in a traditional diffusion process for the case $L_p<r_a$ (figure 2(a),(c),(e)). However, for $L_p>r_a$, a quasi-linear decrease in z direction occurs (figure2g).

For large v_r values, the distribution of the charge carriers depends both on the r and z directions, and the diffusion process is no more quasi-one dimensional. Along the radial direction r, the decrease of the $p(r,z)$ concentration from the wire axis to its surface is about a factor of two. The extension of the generated charge carriers along the z direction (i.e. along the wire axis) is located near generation volume. The decrease has an exponential shape similar to a traditional diffusion.

3.2 The EBIC signal

3.2.1 Effect of the diffusion length on the EBIC signal

Diffusion length is defined as the average distance travelled by charge carriers before being recombined. This parameter is of great importance for the solar cell performance. If this distance is long, even the carriers generated in the neutral regions far from the p-n junction are collected and contribute to the photovoltaic conversion. The increase of the diffusion length results in a broader spreading of the collected EBIC current, which however depends on the surface recombination velocity as illustrated in figure 3.

In the neutral regions of the junction, the EBIC signal increases with the decreasing of the distance between theprobe and the junction position.

The signal reaches its highest value when the probe is focused on the edge of the space charge region (either on the p or n side).In this case, electron-hole pairs are generated in a region very close to the junction, so the chance of being collected is high. For the case of low values of v_r (figure 3(a)), the EBIC signal increases with the increase in L in a similar manner to that of the bulk case.This proves that the effect of the recombination of charge carriers on the lateral surface of the wire is negligible and the diffusion is mainly one-dimensional in z direction in neutral regions.For the case of high v_r values (figure 3(b)), the signal away from the space

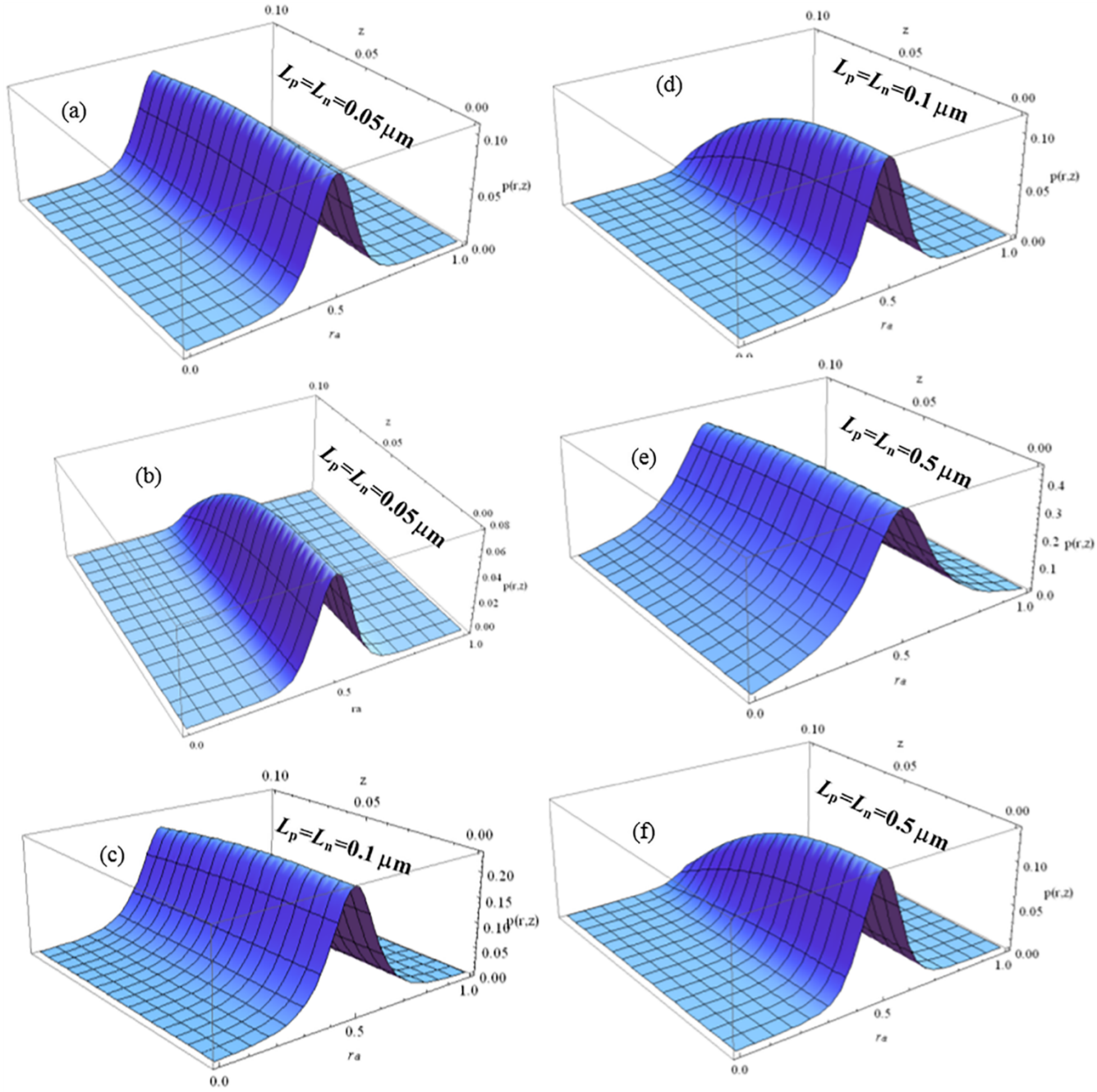

Figure 2. The 2D (axial and radial) normalized distribution of excess carriers in the n region for different diffusion length values and for a low and a hight surface recombination velocity. E_0 =5 keV, r_a=0.1 µm, NW length h=2 µm, the beam position $z_0 = 0.5d_1$ (i.e. z_0 is at the midle of the n region). (a, c, e panels) $s_p=s_n=100$ µm^{-1},(b, d, f panels) $s_p=s_n=10$µm^{-1}.

charge region decreases considerably, and it only weakly depends on the diffusion length.This confirms that when the recombination rate of charge carriers at the lateralsurface is very high, the distribution of charge carriers remains confined in the region close to the generation volume. The difference between the curves in the vicinity of the space charge region decreases with the increase of L for the two studied cases, a saturation of the EBIC signal is obtained for a certain value of L. In the SCR, in principle, the EBIC signal is expected to be independent of the L and s values.

However, since the excitation volume can be broader than the space charge region, there are charge carriers generated outside this volume which participate in the formation of the EBIC signal. So, an increasing of EBIC current within this region is noticed. This increase in EBIC current depends on the L and s values and is more pronounced for high acceleration voltages.

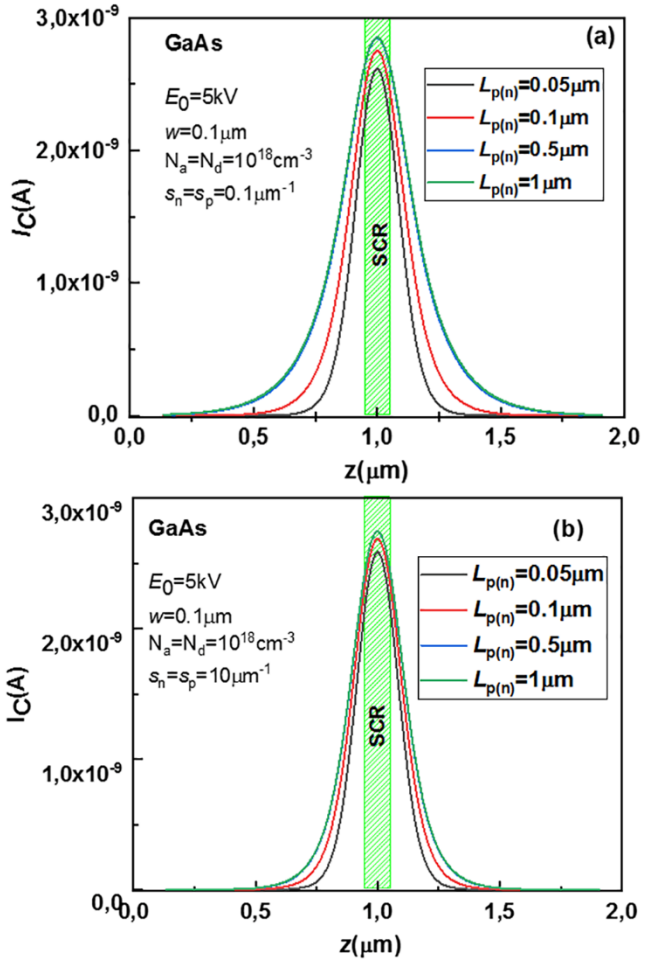

Figure 3. Variation of the EBIC signal for different $L_{p(n)}$ values. r_a=0.1 μm, h= 2μm. E_0=6 keV, (a) s_n=s_p=0.1μm^{-1}, (b) s_n=s_p=10μm^{-1}.

3.2.2 Effect of the surface recombination velocity

Because of the high surface to volume ratio for the nanowire geometry (i.e. large lateral surface), we expect the surface recombination velocity to have a remarkable effect on the collected EBIC signal. Figure 4(a) and (b) show the effect of this parameter on the calculated EBIC signal for the case of $L>r_a$ and $L<r_a$, respectively.

Overall, the EBIC signal outside the space charge region decreases with the increase of the surface recombination velocity and a strong dependence of the EBIC signal on this parameter is observed in the case of $L>r_a$ (figure 4(a)). This proves that the diffusion of charge carriers is no longer one-dimensional and a large part of these generated carriers are diffused to the lateral surface where they are trapped. For the $L<r_a$ case, the EBIC signal is almost independent of the recombination velocity value (figure 4(b)) and decreases rapidly outside the space charge region along the length of the wire (i.e. in the z direction). This shows that the generated charge carriers remain confined to the vicinity of the generation volume.

3.2.3 Effect of the wire radius

Figure 5 shows the effect of the wire radius on the computed EBIC current. The scanning probe is fixed at the middle of the neutral n-doped region ($z=d_1/2$). The EBIC signal increases with the increase of ra. This result could be explained by the fact that when r_a increases the effect of recombination on the lateral surface decreases (more charge carriers are generated in regions far from the wire surface), therefore, the diffusion process is controlled by the bulk recombination of the electron-hole pairs. In addition, the areas of the collection planes at $z=d_1$ and $z=d_2$ increase with the increase of r_a which results in an increase in EBIC signal according to equations 13 and 14. For large value of r_a, the EBIC signal becomes independent of this parameter which means that the quasi-bulk situation is reached (the pure bulk case corresponds to infinitely large r_a).

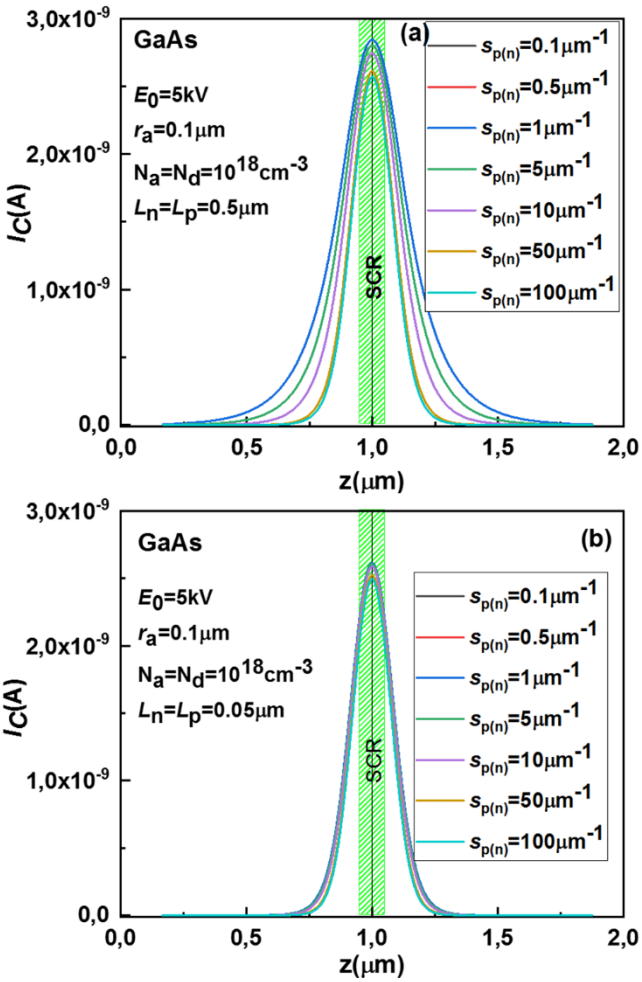

Figure 4. Variation of the EBIC signal for different values of surface recombination velocity r_a=0.1 μm, h= 2μm. E_0=5keV. (a) L_n=L_p=0.5μm, (b) L_n=L_p=0.05μm.

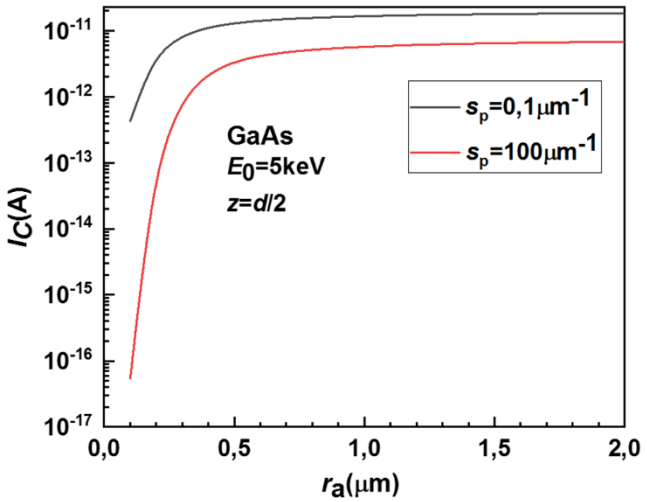

Figure 5. Variation of the EBIC signal versus the radius r_a for h= 2 μm. E_0=5 keV, L_n =0.1μm, and z= d_1/2. s_n=0.1 μm^{-1}(*black line*), s_n= 100 μm^{-1}(*red line*)

3.2.4 Verification of the model

To check the validity of the model, we have reproduced several experimental EBIC profiles of axial p-n junctions taken from different publications and determined their electrical parameters (the diffusion length and the charge carriers surface recombination velocity). First, we have reproduced experimental points of a GaAs axial p-n junction nanowire with a diameter of 200 nm from the publication by Gutsche et al [17] with and without surface treatment using ammonium sulfide. This treatment is reported to result in surface passivation. For the treated case, we have taken the EBIC profile of the diode measured after 96 h after the treatment. We refer as "diode1", and "diode2", to the diode without and with surface passivation, respectively. The results are displayed in figure 6(a). In addition, we have also reproduced the EBIC profile oftwo GaAs axial p-n junctionswith different diameterstaken from Darbandiandand Watkins [16].

We name "diode 3", the diode with a nanowire diameter of 420 nm, and "diode 4" those with a nanowire diameter of 520 nm. The simulation results are presented in figure 6(b). Finally, we have reproduced the EBIC profile of a GaAsP axial p-njunction nanowire of 100 nm of diameter taken from Saket et al [15]. This latter is referred to as "diode 5". The extracted values of diffusion lengths and surface recombination velocities obtained from these analyses and the original onesreported in the corresponding publications are presented in Table 1. Their calculated and modelled EBIC profiles are presented on figure 6(a), (b) and (c), respectively. The extracted parameters obtained with our model are different from those obtained in the original publications. This difference is due to the fact that the authors of those works had extracted the diffusion length of charge carriers from their EBIC profiles using a simplified diffusion model yielding an exponential law, while our model more rigorously accounts for the surface recombination and 3D carrier diffusion. This comparison clearly illustrates the importance of taking into account the surface recombination in EBIC profile modeling.

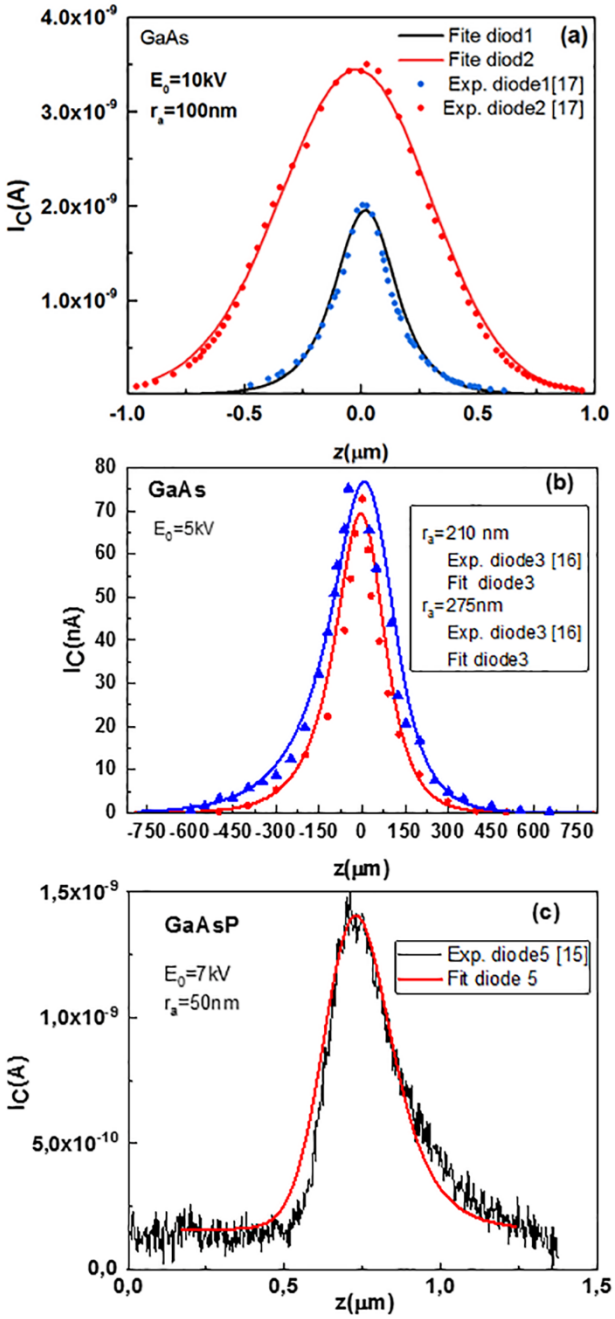

Figure 6. Fit of the EBIC profiles of Axial-pn junction nanowires. (a) GaAs NW diode with r_a=200 nm with and without surface treatment. (b) GaAs NW diode with r_a=210nm and 275 nm. (c) GaAsP NW diode with r_a=50 nm.

Table 1. The values of the diffusion length and of the surface recombination velocity of charge carriers extracted using the present model and those reported in the original publications.

Present work					Previous work			
	L_p(μm)	L_n(μm)	v_{rp}(cm/s)	v_{rn}(cm/s)	L_p(μm)	L_n(μm)	v_{rp}(cm/s)	v_{rn}(cm/s)
Diode 1	0.38	0.55	$4\ 10^5$	$3\ 10^5$	0.13*	0.15*	$4\ 10^6$	$3\ 10^5$
Diode 2	0.6	0.75	$1\ 10^5$	$1\ 10^5$	0.153*	0.173*	-	-
Diode 3	0.1	0.15	$3\ 10^6$	$5\ 10^6$	0.12**	0.11**	$4.7\ 10^5$ **	$3\ 10^6$ **
Diode 4	0.11	0.2	$3\ 10^6$	$5\ 10^5$	0.12**	0.11**	$4.7\ 10^5$ **	$3\ 10^6$ **
Diode 5	0.35	0.05	$2\ 10^5$	$1.5\ 10^6$	0.56***	0.187***		

(*) ref[17], (**) ref[16] and (***) ref[15]

4. Conclusion

In this paper, we have proposed a mathematical model that allows for a quantitative modeling of the EBIC experiments for the case of axial nanowire p-n junctions having different surface recombination velocities. The model allows to simultaneously extract the diffusion length value of minority charge carriers and the corresponding surface recombination velocity.

The effect of the beam and the nanowire parameters on the EBIC signal is illustrated.

The results show that surface recombination v_r affects the spatial distribution of charge carriers and hence the collected current. For the case where L is less than r_a, the collected EBIC current is quasi-independent of the v_r value and the bulk recombination process is the predominant recombination process. However, for the case where L is greater than r_a, the collected EBIC current depends on v_r: it decreases with the increase of the v_r value. In this case the surface recombination process is the dominant recombination process. For large v_r values, the EBIC profile is independent of this parameter.

Overall, the EBIC profile increases with the increase of the L value till a critical value L_c where it becomes independent of this parameter. The EBIC signal increases with r_a, due to the increase in the collection surfaces. For very large values of r_a, the EBIC signal is independent of this parameter.

In general, the use of a bulk EBIC model to extract the diffusion length values of charge carriers for the case of nanowire junctions is justified only for low surface recombination velocities (i.e. for nanowires with a good passivation of the lateral surface). However, the use of these models for the case of a high surface recombination velocity can lead to a wrong estimation of the extracted L values, which are underestimated, since the diffusion and the EBIC profiles strongly depend on this parameter. This effect is illustrated by modeling of the published experimental data.

Acknowledgements

The authors thank O. Saket and V. Piazza for providing illustrations of the experimental EBIC configuration shown in Figure 1, the EBIC setup belongs to the facilities of RENATECH, the French National Nanofabrication Network. The financial support from the EU EMPIR Euramet project "NanoWires" (grant no. 19ENG05) and from the ANR "Napoli" (ANR-18-CE24-0022) and the ANR SCENIC (ANR-20-CE09-0005) are acknowledged.

Data availability statement

The data that support the findings of this study are available upon reasonable request from the authors.

Conflicts of interest

There are no conflicts of interest

ORCID iDs

Abderrezak Lahreche https://orcid.org/0000-0003-3715-9667
Andrey V. Babichev https://orcid.org/0000-0002-3463-4744
Maria Tchernycheva https://orcid.org/0000-0003-4144-0793

References

[1] Goktas N I, Wilson P, Ghukasyan A, Wagner D, McNamee S and LaPierre R R 2018 Nanowires for energy: A review *Appl. Phys. Rev.* **5** 041305

[2] Haverkort J E M, Garnett E C and Bakkers E P A M 2018 Fundamentals of the nanowire solar cell: Optimization of the open circuit voltage *App. Phys. Rev.* **5** 031106

[3] Otnes G and Borgström M T2017 Towards high efficiency nanowire solar cells *Nano Today* **12** 31–45

[4] Piazza V, Mancini L, Chen H-L, Collin S and Tchernycheva M 2018 Nanoscale Analyses Applied to Nanowire Devices, book chapter in "Semiconductors and Semimetals" **98** 231.

[5] Abou-Ras D and Kirchartz T 2019 Electron-Beam-Induced Current Measurements of Thin-Film Solar Cells *ACS Appl. Energy Mater.* **2** 6127–39

[6] Haney P M, Yoon H P, Koirala P, Collins R W and Zhitenev N. B 2014 *IEEE 40th Photovoltaic Specialist Conference* 14683485

[7] Haney P M, Yoon H P, Gaury B and Zhitenev N B 2016 Depletion region surface effects in electron beam induced current measurements *J. Appl. Phys.* **120** 095702

[8] Kedem N, Brenner T M, Kulbak M, Schaefer N, Levcenko S, Levine I, Abou-Ras D, Hodes G and Cahen D 2015 Light-Induced Increase of Electron Diffusion Length in a p–n Junction

Type $CH_3NH_3PbBr_3$ Perovskite Solar Cell *J. Phys. Chem. Lett.* **6** 2469−76
[9] Nichterwitz M, Caballero R, Kaufmann C A, Schock H-W and Unold T 2013 Generation-dependent charge carrier transport in Cu(In,Ga)Se_2/CdS/ZnO thin-film solar-cells *J. Appl. Phys.* **113** 044515
[10] Moore J E, Affouda C A, Maximenko S I and Jenkins P 2018 Analytical and numerical simulation of electron beam induced current profiles in pn junctions *J. Appl. Phys.* **124** 113102
[11] Higuchi H and Tamura H 1965 Measurement of the lifetime of minority carriers in semiconductors with a scanning electron microscope *Jpn. J. Appl. Phys.* **4** 316
[12] Berz F and Kuiken H K 1976 Theory of life time measurements with the scanning electron microscope: Steady state *Sol. Stat. Elec.* **19** 437–45
[13] Ong V K S, Hang J C H and Chan D S H 1994 A direct and accurate method for the extraction of diffusion length and surface recombination velocity from an EBIC line scan *Sol. Stat. Elect.* **37** 1–7
[14] Gao Q, Fu L, Li L, Vora K, Li Z, Wang F, Li Z, Wenas Y, Mokkapatil S, Karouta F, Tan H H and Jagadish C 2015 Direct Characterization of Axial p-n Junctions for InP Nanowire Array Solar Cells Using Electron Beam-Induced Current, in Light, Energy and the Environment 2015, OSA Technical Digest (online) (Optical Society of America, 2015), paper PTu3B.4
[15] Saket O, Himwas C, Piazza V, Bayle F, Cattoni A, Oehler F, Patriarche G, Travers L, Collin S, Julien F H, Harmand J-C and Tchernycheva M 2019 Nanoscale electrical analyses of axial-junction GaAsP nanowires for solar cell applications *Nanotechnology* **31** 145708
[16] Darbandi A and Watkins S P 2016 Measurement of minority carrier diffusion lengths in GaAs nanowires by a nanoprobe technique *J. Appl. Phys.* **120** 014301
[17] Gutsche C, Niepelt R, Gnauck M, Lysov A, Prost W, Ronning C and Tegude F-J 2012 Direct determination of minority carrier diffusion lengths at axial GaAs nanowire p–n junctions *Nano Lett.* **12** 1453–58
[18] Piazza V, Wirths S, Bologna N, Ahmed A A, Bayle F, Schmid H, Julien F and Tchernycheva M 2019 Nanoscale analysis of electrical junctions in InGaP nanowires grown by template-assisted selective epitaxy *Appl. Phys. Lett.* **114** 103101
[19] Zhong Z, Li Z, Gao Q, Li Z, Peng K, Li L, Mokkapati S, Vora K, Wu J, Zhang G, Wang Z, Fu L, Tan H H and Jagadish C 2016 Efficiency enhancement of axial junction InP single nanowire solar cells by dielectric coating *Nano Energy* **28** 106–14
[20] Yang M, Dvorak D, Leistner K, Damm C, Watkins S P and Kavanagh K L 2018 Axial EBIC oscillations at core/shell GaAs/Fe nanowire contacts *Nanotechnology* **30** 025701
[21] Chen C Y, Shik A, Pitanti A, Tredicucci A, Ercolani D, Sorba L, Beltram F and Ruda H E 2012 Electron beam induced current in InSb-InAs nanowire type-III heterostructures *Appl. Phys. Lett.* **101** 063116
[22] Tchoulfian P, Donatini F,Levy F, Dussaigne A, Ferret P and Pernot J 2014 Direct imaging of p–n junction in core–shell GaN wires *Nano Lett.* **14** 3491–98
[23] Fang Z, Donatini F, Daudin B and Pernot J 2018 Axial p–n junction and space charge limited current in single GaN nanowire *Nanotechnology* **29** 01LT01
[24] Tchernycheva M, Neplokh V, Zhang H, Lavenus P, Rigutti L, Bayle F, Julien F H, Babichev A, Jacopin G, Largeau L, Ciechonski R, Vescovi G and Kryliouk O 2015 Core–shell InGaN/GaN nanowire light emitting diodes analyzed by electron beam induced current microscopy and cathodoluminescence mapping *Nanoscale* **7** 11692–701
[25] Dan Y, Seo K, Takei K, Meza J H, Javey A and Crozier K B 2011 Dramatic reduction of surface recombination by in situ surface passivation of silicon nanowires *Nano Lett.* **11** 2527–32
[26] Saket O, Himwas C, Piazza V, Bayle F, Cattoni A, Oehler F and Patriarche G 2020 Nanoscale electrical analyses of axial-junction GaAsP nanowires for solar cell applications *Nanotechnology* **31** 145708
[27] Bonard J M and Ganiere J D 1996 Quantitative analysis of electron-beam-induced current profiles across p–n junctions in GaAs/$Al_{0.4}Ga_{0.6}As$ heterostructures *J. Appl. Phys.* **79** 6987
[28] Kanaya K and Okayama S 1972 Penetration and energy-loss theory of electrons in solid targets *J. Phys. D: Appl. Phys* **5** 43
[29] Morse P M and Feshbach H 1953 Methods of Theoretical Physics, McGraw-Hill, New York